

Numerical Analysis of Raised Cosine Sampled Chirped Bragg Grating for Dispersion Compensation in Dense Wavelength Division Multiplexing Systems

FETHALLAH KARIM*, OMAR SEDDIKI
Laboratory of Telecommunications, Faculty of Engineering Sciences
Aboubekr Belkaid University
13000 Chetouane Tlemcen ALGERIA
*Corresponding author email: karim_fethallah@live.fr

Abstract— In this paper, a numerical investigation of raised-cosine sampled chirped fiber Bragg grating (SCFG) has been presented. This multi channel filter is modeled by coupled mode theory and simulated by transfer matrix method. The optical period changes linearly at each section of the grating according to a negative period variation. To reduce ripples and side lobes, a raised-cosine apodization is applied. SCFG is proposed for the purpose of dispersion management in dense wavelength division multiplexing systems. Numerical results show that SCFG presents five channels in a bandwidth of 0.6 nm and with a dispersion of -1400 ps/nm. The wavelength spacing between two neighboring channels is 0.8 nm.

Keywords— Sampled chirped fiber grating, dispersion compensation, wavelength division multiplexing.

I. INTRODUCTION

Degradation of transmitted signals due to chromatic dispersion is one of the major limiting factors in long haul optical communication links, since transmission rates are constantly increasing and the loss of optical fiber becomes lower. Several techniques have been proposed to achieve dispersion compensation and pulse recompression as prechirped pulse transmission or dispersion shifted fibers. However, the first one does not cancel the dispersion completely, and the second one requires modifying existing fiber links. In recent years, there has been increasing interest in dispersion compensating fiber Bragg gratings because they are entirely passive and their size, cost and fiber compatibility make them very attractive devices [1].

The chirped fiber grating (CFG) has been successfully used to provide the necessary dispersion compensation in dispersed managed systems. However, in a wavelength division multiplexing (WDM) system, each channel must have its own CFG for dispersion compensation. The sampled chirped fiber grating (SCFG) [2] has brought forward. Comparing with

CFG, it has the same length, but can compensate several WDM channels simultaneously. SCFG has a great prospect for dispersion compensation.

II. THEORY AND FUNDAMENTALS OF FIBER BRAGG GRATINGS

The feasibility of fabricating refractive index grating was discovered and reported by Hill *et al.* in 1978 [3]. Subsequently, Meltz *et al.* devised a method to control the fabrication of grating using UV laser [4]. Basically, when a germanium-doped silica core fiber is exposed to ultraviolet (UV) radiation (with wavelength around 240 nm), it results in a permanent change in the refractive index of the germanium-doped region, due to the photosensitivity nature of the fiber and, using such an exposure, it is possible to obtain refractive index changes by factors as large as 10^{-3} in germanium-doped silica fiber. If the fiber is exposed to a pair of interfering UV beams as shown in Fig.1, then in regions of constructive interference which correspond to high UV intensity, the local refractive index will increase [5].

At the same time, in regions of destructive interference, here the intensity of UV light is negligible, there is no index change. Therefore, an exposure to an interference pattern will result in a periodic refractive index modulation along the length of the fiber, the period of modulation being exactly equal to the spacing between the interference fringes [5]. Refractive index modulation is represented by [6]

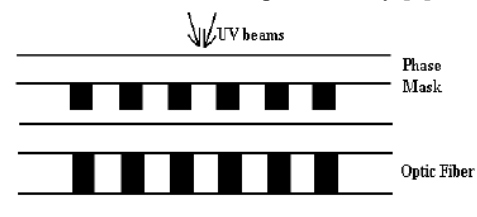


Fig. 1. UV beams on optical fiber through a phase mask

$$n(x, y, z) = \bar{n}(x, y, z) + \delta n(x, y, z) \cos\left(\frac{2\pi}{\Lambda} z + \varphi(z)\right) \quad (1)$$

Where $\bar{n}(x, y, z)$ is the average refractive index of the core, $\delta n(x, y, z)$ is the modulation of the refractive index, Λ is the Bragg period and $\varphi(z)$ is the grating phase.

A small amount of incident light is reflected at each periodic refractive index change. The entire reflected light waves are combined into one large reflection at a particular wavelength when the strongest mode coupling occurs. This is referred to as the Bragg condition, and the wavelength at which this reflection occurs is called the Bragg wavelength. Only those wavelengths that satisfy the Bragg condition are affected and strongly reflected. The reflectivity of the input light reaches a peak at the Bragg wavelength. The Bragg grating is essentially transparent for incident light at wavelengths other than the Bragg wavelength where phase matching of the incident and reflected beams occurs [7]. Bragg wavelength λ_B is given by [7]

$$\lambda_B = 2n_{\text{eff}} \Lambda \quad (2)$$

Where n_{eff} is the effective refractive index. This is the condition for Bragg resonance. From equation (2), we can see that the Bragg wavelength depends on the refractive index and the grating period [7].

The effective refractive index n_{eff} and Bragg period Λ are constant for the uniform Bragg grating. Fig. 2 shows the reflectance of the uniform Bragg grating, with the following parameters: $n_{\text{eff}} = 1.447$, $L = 1$ cm, $\delta n = 0.0004$.

The fiber Bragg grating has the advantages of a simple structure, low insertion loss, high wavelength selectivity, polarization insensitivity and full compatibility with general single mode communication optical fibers [8].

III. MODELING OF FIBER BRAGG GRATING

We have chosen Coupled Mode Theory (CMT) for the analysis and modeling of fiber Bragg gratings because it is straight forward, intuitive and one of the most important tools to understand the main optical properties of gratings. Besides,

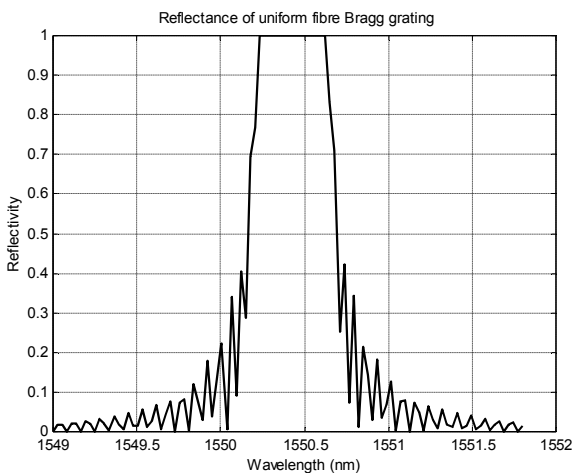


Fig.2. Reflectance of uniform fibre Bragg grating

it gives quantitative information about diffraction efficiency and spectral dependence of fiber gratings and can model with a high level of accuracy the optical properties of interest [9].

The CMT theory leads to a pair of differential coupled equations that define the reflectivity of the structure, that can be computed following two different approaches, direct numeric integration or piecewise-uniform techniques. We have chosen the second one, known as Transfer Matrix Method, because it is simple to implement, provides sufficient accuracy and it is the fastest method, what is a very important constraint in this type of modeling applications [9].

The basic idea of the coupled-mode theory is that the electrical field of the waveguide with a perturbation can be represented by a linear combination of the modes of the field distribution without perturbations.

The transverse component of the electric field at position z in the perturbed fiber can be described by a linear superposition of the ideal guided modes of the unperturbed fiber, which can be written as [6]

$$\vec{E}_t(x, y, z, t) = \sum_j [E_j(x, y, z, t) + E_{-j}(x, y, z, t)] \quad (3)$$

The coupling coefficient $k(z)$ and the local detuning $\hat{\sigma}(z)$ are two important parameters in the coupled mode equations [10]. They are fundamental parameters in the calculation of the spectral response of the fiber Bragg gratings. The general (DC) self coupling coefficient $\hat{\sigma}(z)$ can be represented by [10]

$$\hat{\sigma} = \delta + \frac{2\pi}{\lambda} \delta n_{\text{eff}} - \frac{1}{2} \frac{d\varphi}{dz} \quad (4)$$

Where $\frac{1}{2} \frac{d\varphi}{dz}$ describes a possible chirp of the grating period,

φ is the grating phase and δn_{eff} is the refractive index change.

The detuning δ is represented by [10]

$$\delta = 2\pi n_{\text{eff}} \left(\frac{1}{\lambda} - \frac{1}{\lambda_D} \right) \quad (5)$$

Where λ_D is the design wavelength for Bragg reflectance.

The coupling coefficient $k(z)$ is written by [10]

$$k(z) = \frac{\pi}{\lambda} \delta n_{\text{eff}} g(z) \nu \quad (6)$$

Where $g(z)$ is the apodization function, and ν is the fringe visibility.

A non-uniform fiber Bragg grating can be divided into many uniform sections along the fiber. The incident light wave propagates through each uniform section i that is described by a transfer matrix F_i . For the structure of the fiber Bragg grating, the matrix F_i can be described as [10]

$$F_i = \begin{bmatrix} \cosh(\gamma_B dz) - i \frac{\hat{\sigma}}{\gamma_B} \sinh(\gamma_B dz) & -i \frac{k}{\gamma_B} \sinh(\gamma_B dz) \\ i \frac{\hat{\sigma}}{\gamma_B} \sinh(\gamma_B dz) & \cosh(\gamma_B dz) + i \frac{\hat{\sigma}}{\gamma_B} \sinh(\gamma_B dz) \end{bmatrix} \quad (7)$$

Where k is described by equation (6), $\hat{\sigma}$ is described by equation (4) and γ_B is represented by [11]

$$\gamma_B = \sqrt{k^2 - \hat{\sigma}^2} \quad (k^2 > \hat{\sigma}^2) \quad (8)$$

$$\gamma_B = i\sqrt{\sigma^2 - k^2} \quad (k^2 < \sigma^2) \quad (9)$$

A. Group delay and dispersion

The group time delay and dispersion of the grating can be obtained from the phase information of the reflection coefficient.

The delay time τ_p for light reflected in a grating is defined as follows [10]

$$\tau_p = \frac{d\theta_p}{d\omega} = -\frac{\lambda^2}{2\pi c} \frac{d\theta_p}{d\lambda} \quad (10)$$

The dispersion d_p (in ps/nm) is defined as follows [10]

$$d_p = \frac{d\tau_p}{d\lambda} = \frac{2\tau_p}{\lambda} - \frac{\lambda^2}{2\pi c} \frac{d^2\theta_p}{d\lambda^2} \quad (11)$$

IV. CHIRPED FIBER BRAGG GRATING

A chirped Bragg grating is a grating that has a varying grating period. There are two variables that can be changed to obtain a chirped grating: one is to change the Bragg period; another is to change the refractive index along the propagation direction of the fiber.

Fig. 3 shows a linear chirped Bragg grating. In this case, the period of the grating varies linearly with the position. This makes the grating reflect different wavelengths (or frequencies) at different points along its length. Changing the refractive index has the same effect as changing the period along the z -direction. This means the optical period is changed even though the physical period of the grating is fixed. So these two variables can be merged, and described by one variable.

Fig. 4 shows a chirped grating, designed from N sections each one with different chirp. The length of each section δl depends on the total length of the grating and the number of sections. In our work, the refractive index is changed in each section linearly.

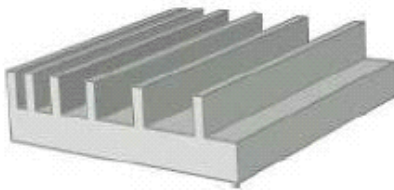


Fig.3. Linear chirped Bragg grating

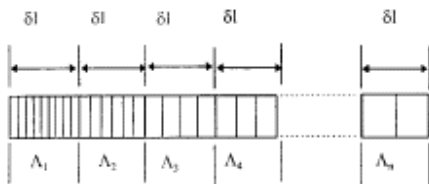


Fig.4. Chirped grating with linear change in the refractive index

The phase term in equation (4) for a linear chirped grating is [10]

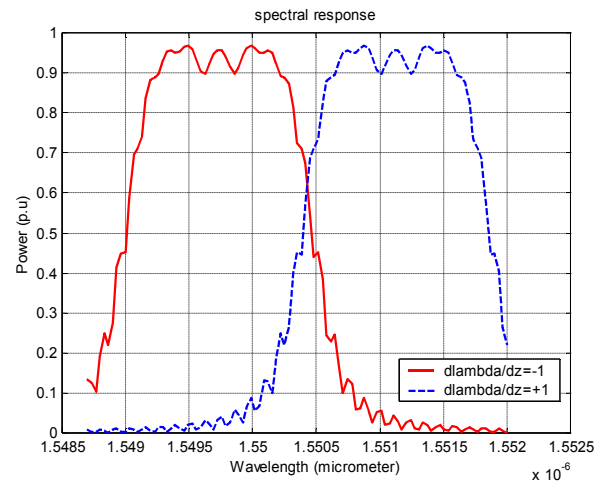
$$\frac{1}{2} \frac{d\varphi}{dz} = -\frac{4\pi \times n_{eff} \times b}{\lambda_d^2} \times \frac{d\lambda_d}{dz} \quad (12)$$

Where $\frac{d\lambda_d}{dz}$ is the chirp variable, and b is the rate of change of the refractive index in each section.

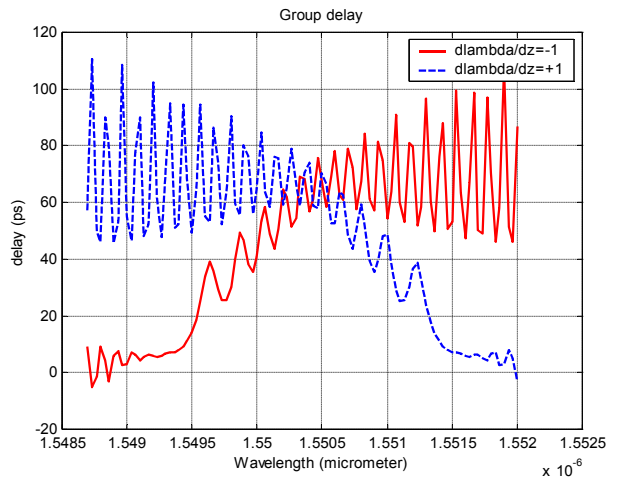
Fig. 5 shows the reflectivity and time delay of two chirped gratings with changed chirp variable $\frac{d\lambda_d}{dz}$. If the chirp variable

is positive, the period of the linear chirped grating increases along the propagation direction. On the other hand, if it is negative, the period of the linear chirped grating reduces along the propagation direction.

In a fiber with negative period variation (negative dispersion), we remark that higher wavelength penetrates into the grating more deeply and delays more time after to be reflected. Therefore, in a fiber with positive dispersion higher wavelength makes a short delay to be reflected at each section of the grating.



(a) Reflectivity



(b) Time delay

Fig.5. Two linear chirped gratings with an equal chirp and opposite chirp variables

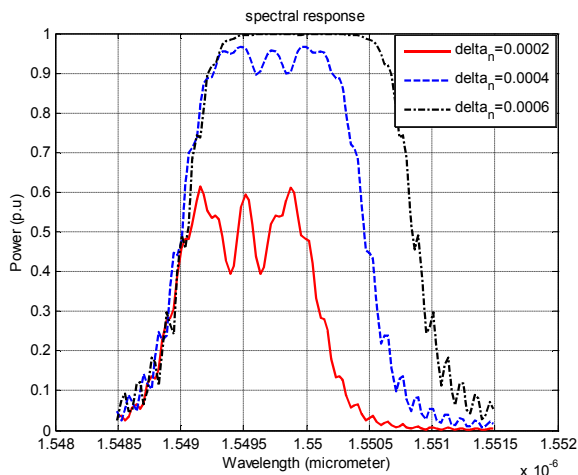


Fig. 6. Reflectivity spectrum of three chirped gratings with different refractive index change

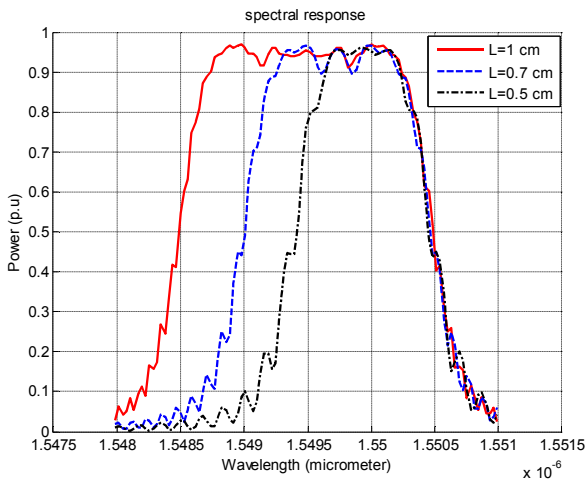


Fig. 7. Reflectivity spectrum of three chirped gratings with different total length

To increase the bandwidth of a grating (i.e negative dispersion) and at the same time the reflectivity peak, we should increase the refractive index change δn_{eff} (Fig. 6). Another solution for increasing the negative dispersion of a chirped grating by keeping the reflectivity peak constant; is to increase its total length (Fig. 7).

V. APODIZED FIBER BRAGG GRATING

The refractive index change is constant in uniform fiber Bragg gratings. The reflectance spectrum of a finite-length Bragg grating with a uniform modulation of the refractive index is accompanied by a series of side lobes at the adjacent wavelengths. It is very important to minimize and, if possible, eliminate the reflectivity of these side lobes [12].

From all figures showed above, we remark that the reflectivity spectrum presents side lobes and group delay presents some ripples. These features should be improved for application in communication systems and especially in dispersion compensation applications. One method is by using

apodization [10]. Apodization can be achieved by a contoured exposure to UV light to reduce the refractive index excursions towards both ends of the grating.

The effect of the apodization in the models of the Bragg grating can be represented by using a z -dependent function $g(z)$ in the refractive index [13].

The refractive index of an apodized Bragg grating can be written as

$$n(z) = n_0 + \delta n_0 + \delta n g(z) \cos\left(\frac{2\pi}{\Lambda} z + \varphi(z)\right) \quad (13)$$

Where δn is the depth of the modulation, and $g(z)$ is the modulation function (also called the apodization function). Generally, this function can be gaussian, raised cosine, sinc, blackman, hamming, Kaiser etc. The apodization function is $g(z)=1$ for unapodized Bragg grating.

The raised cosine function has been chosen for the apodization of the coupling coefficient. This function can be written as [10]

$$g(z) = \alpha \left[1 + \cos\left(\frac{\pi\left(z - \frac{L}{2}\right)}{L}\right) \right] \quad (14)$$

Where α is the raised-cosine parameter and L is the total length of the grating. The modulation function is plotted on Fig. 8. We can increase the reflectivity peak and the bandwidth of the spectral response by incrementing the raised cosine parameter α .

Fig. 9 and Fig. 10 illustrate the difference between unapodized and a raised cosine grating. On Fig. 9, we remark side lobes on the spectral response of unapodized grating. With a variable couplage, side lobes were suppressed (Fig. 9 (b)).

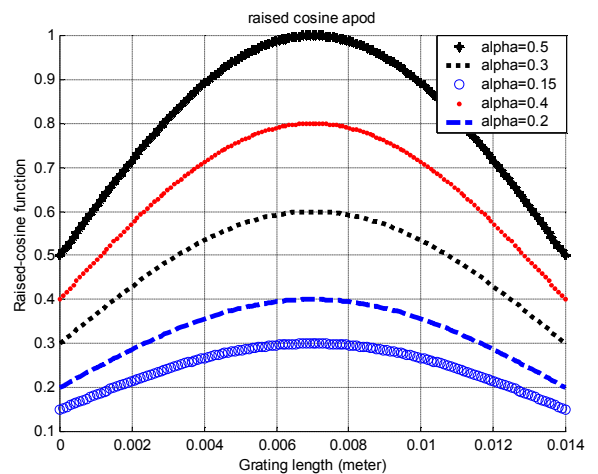
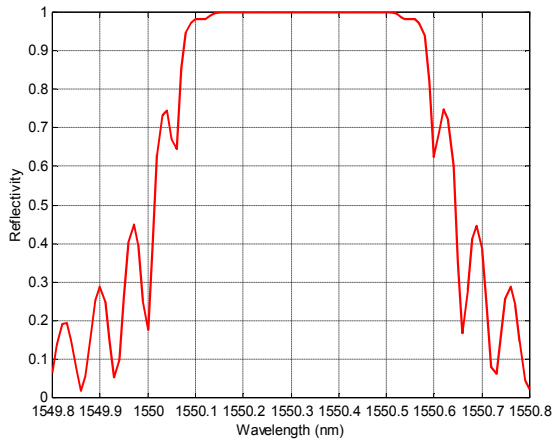
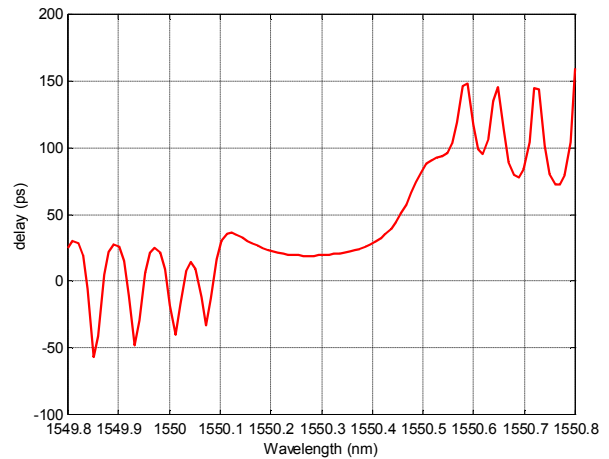


Fig. 8. Raised cosine function

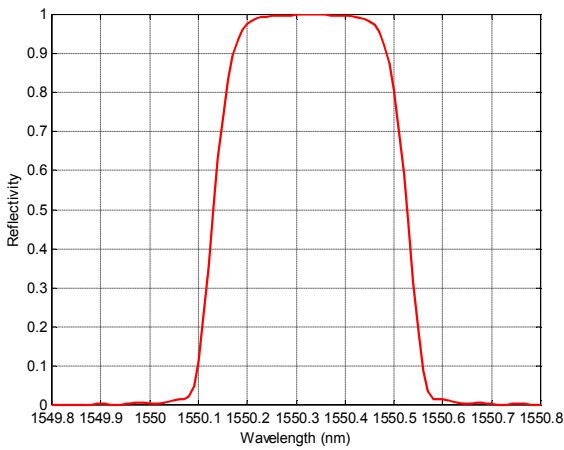


(a) Unapodized grating



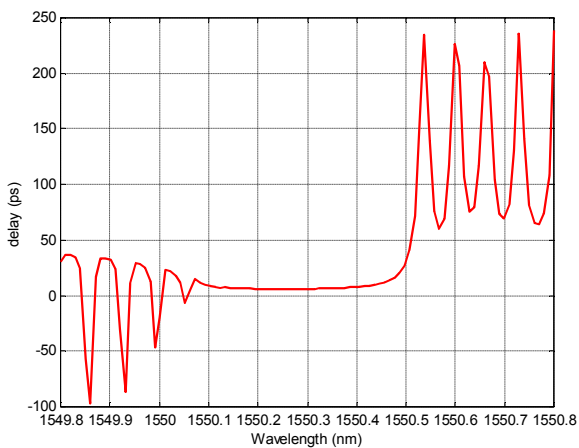
(b) Raised cosine grating

Fig.10. Time delay of unapodized and raised cosine grating



(b) Raised cosine grating

Fig.9. Reflectivity of unapodized and raised cosine grating



(a)Unapodized grating

On the time delay of unapodized grating, ripples higher than 100 ps occur (Fig. 10 (a)). That is not acceptable in optical transmission links because NRZ code in the reception module will contain errors. With a raised cosine apodization ripples are reduced less than 50 ps (Fig. 10 (b)).

VI. SAMPLED FIBER BRAGG GRATING

A. Principle

Fig. 11 is a schematic representation of a sampled grating structure, where L_A is the sampling period and L_B is the range that was exposed by UV light. We define the duty cycle, R , which is the ratio between the section length and the sampling period

$$R = \frac{L_B}{L_A} \quad (15)$$

The range $L_A - L_B$, between two grating sections, is without exposure to UV light. This range can be represented by the phase shift matrix [10]

$$F_{P_i} = \begin{bmatrix} \exp\left(\frac{-i\phi_i}{2}\right) & 0 \\ 0 & \exp\left(\frac{+i\phi_i}{2}\right) \end{bmatrix} \quad (16)$$

Where ϕ_i is the value of the phase shift, it can be written as [10]

$$\phi = \frac{4\pi n_{eff}}{\lambda} \Delta z \quad (17)$$

Where Δz is the separation between two grating sections.

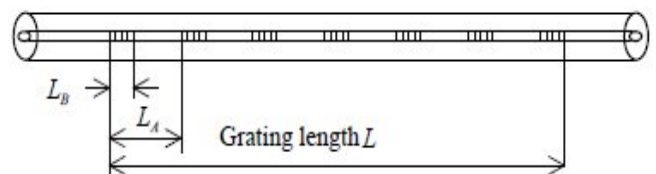


Fig.11. Schematic of sampled grating structure

B. Characteristics of sampled grating

The frequency spacing between two adjacent channels can be written as [2]

$$\Delta f = \frac{c}{2n_{eff}L_A} \quad (18)$$

The channel spacing is defined as follows

$$\delta\lambda = \frac{\lambda^2}{2n_{eff}L_A} \quad (19)$$

Thus, the wavelength between two neighboring channels is only determined exactly by sampling period.

Defining the wavelength range between the first reflection zero point at the two sides of Bragg wavelength as the width of reflectivity, we can get the approximate expression of bandwidth [2]

$$\Delta\lambda = \frac{\Delta n\lambda}{n_{eff}} \sqrt{1 + \left(\frac{\lambda}{\Delta nL_B}\right)^2} \quad (20)$$

Where δn is the refractive index change and L_B is the length of a chirped Bragg section. The channel's number is the quotient of the bandwidth $\Delta\lambda$ and the channel spacing $\delta\lambda$.

Since $\frac{\lambda}{\delta nL_B} \gg 1$, Equation (20) can be rewritten as [2]

$$\Delta\lambda \approx \frac{\lambda^2}{n_{eff}L_B} \quad (21)$$

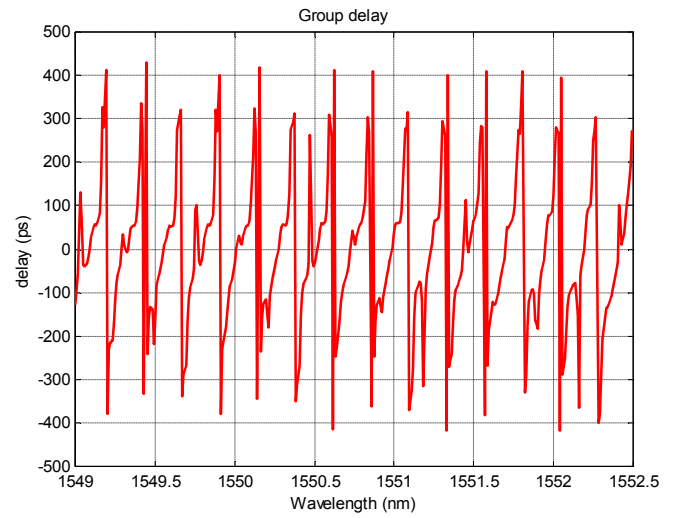
Then, from Equations (18) and (21), the channel number of the sampled grating can be described as [2]

$$m = \frac{2}{R} - 1 \quad (22)$$

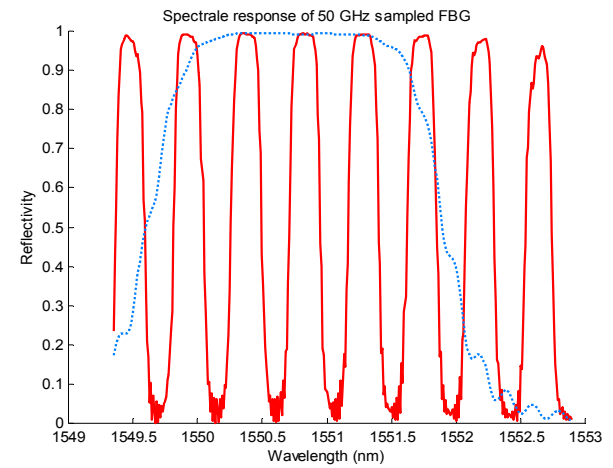
Where R is the duty cycle.

C. Simulation results

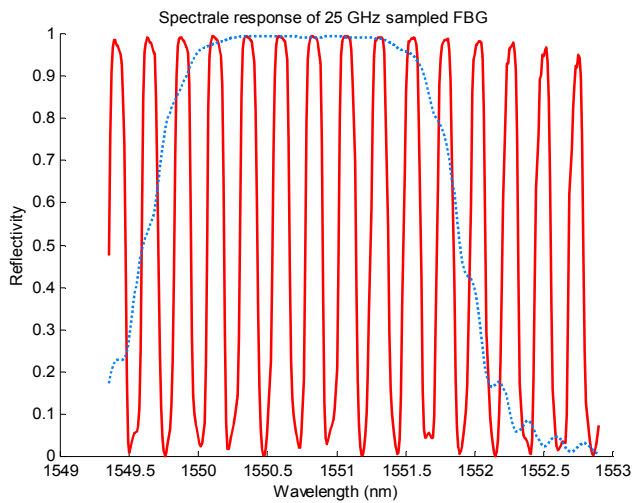
Fig. 12 and 13 show the reflectivity and group delay of raised cosine sampled chirped gratings with the sampling periods of 4.1068 mm and 2.0534 mm respectively.



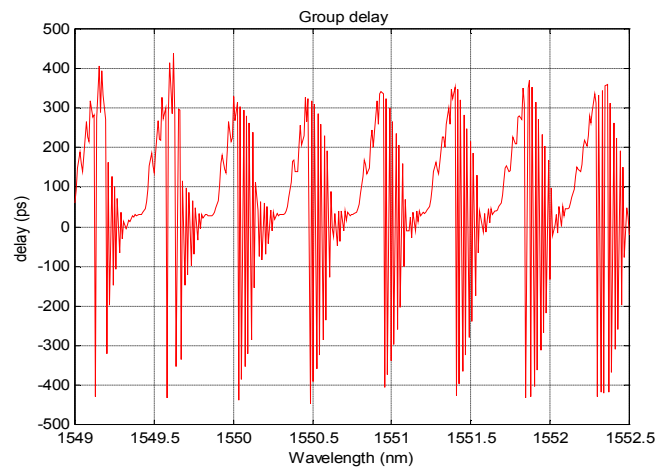
(b) Group delay
Fig.12. Sampled grating with channel spacing of 0.2 nm



(a) Reflectivity



(a) Reflectivity



(b) Group delay
Fig.13. Sampled grating with channel spacing of 0.4 nm

On Fig. 12 the sampled fiber presents ten channels, each one has a bandwidth of 0.25 nm in a total bandwidth of 2.5 nm. When we decrease the sampling period the number of channels decreases automatically, the sampled fiber in the second case presents five channels; each one has a bandwidth of 0.4 nm (Fig. 13). The total length of this grating is 4 mm. We remark that the group delay of each channel increases according to wavelengths, because the variable chirp is negative. The rate of change of optical period in each section, b , equals to 1.1 nm. This chirp permits to increase the total bandwidth of the grating.

Assuming that a single mode fiber presents 17 ps/nm, the designed raised cosine sampled chirped grating should compensate a maximum dispersion of 1445 ps/nm corresponding to an optical transmission link of 85 km. To achieve the compensation of this dispersion, grating channels must have a bandwidth between 0.6 and 0.7 nm.

For a determined optical link, with a specified length L_f and dispersion parameter D_f , we can design a Bragg grating that can achieve the opposite dispersion level of the transmission fiber. The minimum length required to compensate the dispersion introduced by the fiber link is [9]

$$L_0 = \frac{c\Delta\lambda D_f L_f}{2n_{eff}} \quad (23)$$

Where c is the light velocity, n_{eff} is the refractive index of the fiber and $\Delta\lambda$ is the bandwidth to compensate for chromatic dispersion. D_f and L_f are the dispersion and the length of the transmission fiber. In fact, L_0 is the required length for a uniform grating, but for apodized gratings we should use a greater length to compensate the reduction of the coupling strength caused by the apodization profile at the grating ends [1]. Therefore, we can calculate the real or effective length of the grating L_{eff} in function of the apodization profile selected. The effective length is defined as follows [1]

$$L_{eff} = \gamma L_0 \quad (24)$$

Where γ is the apodization factor.

If the condition $\Delta\lambda \leq \Delta\lambda_{chirp}$ is verified, the residual dispersion can be written as [14]

$$D_{resid} = D_f \times L_f + D_g \times L_0 \quad (25)$$

Where $\Delta\lambda_{chirp}$ is the chirped grating bandwidth and D_g is the chirped grating dispersion.

As we have said before, a fiber that has a negative variable chirp presents a negative dispersion. The maximum value of the chirp in the optical period until the last section of the grating equals to 1.1 nm. We note that channel spacing, $\delta\lambda$, is 0.8 nm, thus the sampling period must be 1.0267 mm. To increase the bandwidth of each channel we have decreased the number of channels, by taking the standard frequency spacing of transmission system 100 GHz.

Since the power of each channel decreases as the number of channels increases, it is very difficult to produce fiber Bragg gratings with many channels. In order to compensate the reduction of power, it is necessary to increase refractive index

amplitude modulation δn_{eff} in theoretical limits and if it is not enough, it is necessary to increase the length of the grating.

Fig. 14 shows that a 10 cm of sampled grating, according to the characteristics recapitulated in Table I, presents five channels centered on 1552.34 nm, 1551.52 nm, 1550.7 nm, 1549.88 nm and 1549.05 nm. The reflectivity peak of each channel is about 0.8~0.9 (Fig. 15). Each channel presents a bandwidth of 0.64 nm (Fig. 15).

Fig. 16 shows dispersion spectrum of raised cosine sampled chirped grating. We remark that each channel presents a negative and sufficient dispersion to the compensation of the dispersion of 85 km of a single mode fiber.

Among the five channels, the difference of dispersion is small, showing a good consistence. Numerical results are put in Fig. 17.

Table I. SCFG simulation parameters

L(cm)	10
n_0	1.447
Section's number	300
δn	0.0006
$d\lambda_D/db$ (nm/cm)	-1
b (nm)	1.1
L_A (mm)	1.0267
Raised-cosine parameter	0.15

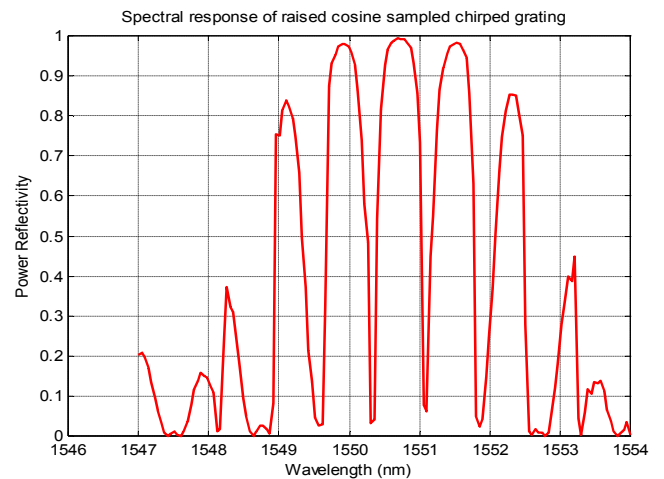


Fig. 14. The reflectivity of raised cosine sampled chirped grating

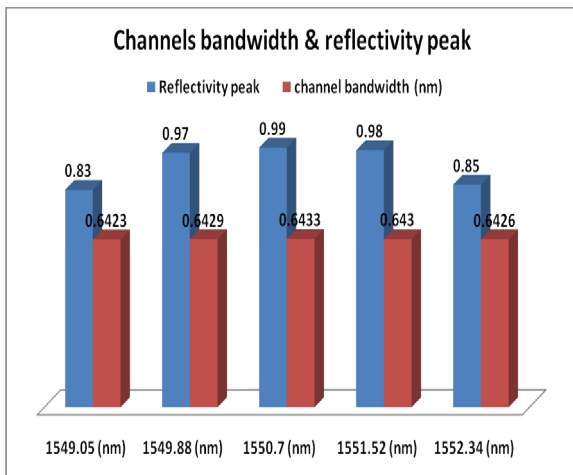


Fig. 15. Simulation results of sampled grating

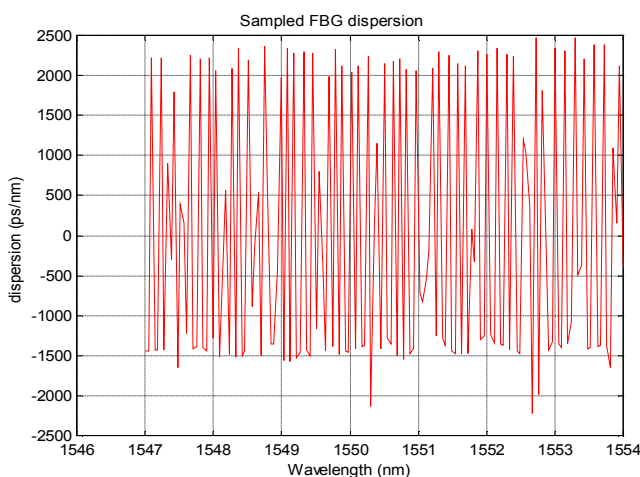


Fig. 16. Sampled grating dispersion

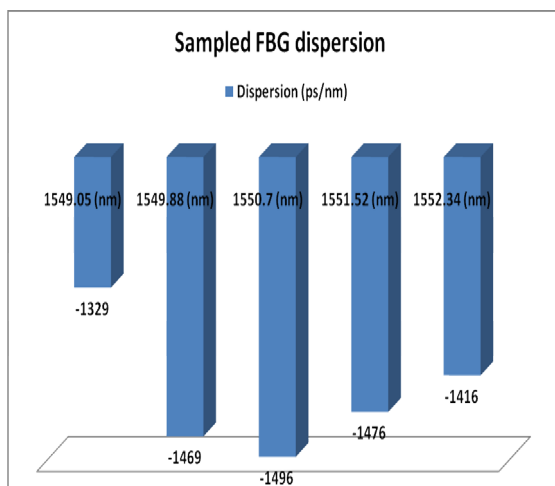


Fig. 17. Simulation results of sampled grating

VII. CONCLUSION

In this paper, the raised-cosine chirped sampled fiber Bragg grating is simulated. The coupled mode theory is a suitable tool to analyze this optical filter. Reflectivity and dispersion spectrum of the multichannel filter with different parameter

values (coupling coefficient, raised-cosine parameter, linear chirp, length of SCFG, sampling period and duty cycle) are simulated and discussed. A raised-cosine apodization is made to reduce group delay ripples and reflectivity side lobes. A linear chirp is applied to the optical period of the grating, resulting in an increased time delay response according to wavelengths. The sampling period is chosen to have the smallest number of channels with the target bandwidth for dispersion compensation.

SCFG gives five channels spaced by 0.8 nm, with a reflectivity peak of 90% and with a dispersion of -1400 ps/nm, in a bandwidth of 0.6 nm. All These characteristics allow using this component in dense wavelength division multiplexing (DWDM) transmission systems as a dispersion compensation module.

REFERENCES

- [1] P. Fernandez, J.C. Aguado, J. Blas, F. Gonzalez, I. DE Miguel, J. Duran, R.M. Lorenzo, E.J. Abril, M. Lopez, "Optimization of the apodization strength for linearly chirped Bragg grating dispersion compensators in optical fiber communications links," *proceeding of the 8th WSEAS Int. Conf on Nanoelectronics and Electromagnetic Compatibility (ICONEMC' 02)*, Skiathos, 2002, pp. 1811-1815.
- [2] C-c.Sun, C-y. Li, X-n. YU, "Study on sampled chirped fiber gratings," *Optics Communication*, vol. 218, pp. 297-302, 2003.
- [3] K.O. Hill, Y. Fujii, D.C. Johnson and B.S. Kawasaki, "Photosensitivity in optical fiber waveguides: Application to reflection filter fabrication," *Applied Physics Lett*, vol. 32, pp. 647-649, 1978.
- [4] G. Meltz, W.W. Morey and W.H. Glenn, "Formation of Bragg gratings in optical fibers by a transverse holographic method," *Optics Lett*, vol 14, pp. 823-825, 1989.
- [5] K.Y. Lee, K.K. Lee, S.L. Ho, "Exploration of using FBG sensor for derailment detector," *proceeding of the 8th WSEAS Int. Conf on Robotics, Distance Learning and Intelligent Communication Systems (ICRODIC' 04)*, Izmir, 2004, pp. 489-480.
- [6] A. W. Snyder, J. D. Love, *Optical Waveguide Theory*, Chapman and Hall, London, 1983, pp. 542.
- [7] A. Othonos and K. Kalli, *Fibre Bragg gratings: fundamentals and applications in telecommunications and sensing*, Artech House, 1999, pp. 189-200.
- [8] C. R. Giles, "Lightwave application of fiber Bragg gratings," *Journal of Lightwave Technology*, vol.15, pp. 1391-1404, 1997.
- [9] P. Fernandez, J.C. Aguado, J. Blas, F. Gonzalez, I. DE Miguel, J. Duran, R.M. Lorenzo, E.J. Abril, M. Lopez, "Design and modeling tool for chromatic dispersion compensation with fiber Bragg gratings," *proceeding of the 8th WSEAS Int. Conf on Signal Processing, Robotics and Automation (ISPR' 02)*, Cadiz, 2002, pp. 1901-1905.
- [10] T. Erdogan, "Fibre grating spectra," *Journal of Lightwave Technology*, vol.15, pp. 1277-1294, 1997.
- [11] Y. Chen, S. Jian, *An introduction to lightwave technology*, China Railway Publishing, 2000, pp. 248.
- [12] A.Othonos, "Fibre Bragg gratings," *Review of Scientific Instruments*, vol.68, pp. 4309-4341, 1997.
- [13] C. Martinez, P. Jouglu, S. Magne, and P. Ferdinand, "Phase plate process for advanced fiber Bragg gratings devices manufacturing," *IEICE Transactions on Electronics*, vol. E83-C, pp. 435-439, 2000.
- [14] R. Kashyap, *Fiber Bragg Gratings*, Optics and Photonics, Academic Press, United Kingdom, 1999, pp.315.